



## RESEARCH ARTICLE

### Targeting Diabetic Wound Healing Through Tissue Regeneration with Silver, Copper, and Zinc Nanoparticles in Streptozotocin-Induced Diabetic Albino Rat Model

Ghulam Murtaza<sup>1&2</sup>, Razia Kausar<sup>2</sup>, Shah Nawaz Sial<sup>3</sup>, Amjad Hameed<sup>4</sup>, Sarmad Rehan<sup>2</sup>, Aneela Kanwal<sup>5</sup> and M. Umar Sharif<sup>2</sup>

<sup>1</sup>Faculty of Veterinary and Animal Sciences, Gomal University, Dera Ismail Khan, KPK, Pakistan. <sup>2</sup>Department of Anatomy, University of Agriculture, Faisalabad, Pakistan.; <sup>3</sup>Department of Comparative Biomedical Sciences, University of Surrey, UK., <sup>4</sup>Nuclear Institute of Agriculture and Biology, Faisalabad, Pakistan. <sup>5</sup>Faisalabad Medical University and Allied Teaching Hospital, Faisalabad, Pakistan

\*Corresponding author: razia.kausar@uaf.edu.pk

#### ARTICLE HISTORY (25-456)

Received: May 06, 2025  
Revised: June 01, 2025  
Accepted: June 14, 2025  
Published online: August 25, 2025

#### Key words:

AgNPs  
CuNPs  
Diabetic Wound  
Nano-Medicine  
Tissue Regeneration  
ZnNPs.

#### ABSTRACT

Diabetic wound healing remains a significant clinical challenge, necessitating the development of more effective therapeutic strategies. In this study, we explored the potential of topically applied, chemically synthesized nanoparticles (NPs) as a novel therapeutic strategy for diabetic wound healing. Specially, we evaluated the efficacy of these NPs based ointments on diabetic wound healing through tissue regeneration, using streptozotocin-induced diabetic albino rat model. For this purpose, thirty-six male albino rats were divided into six groups, T0 (Control Normal, CN), T0 (Diabetic Control, DC), T1 (treated with AgNPs @3mg/ml), T2 (treated with CuNPs @2mg/ml), T3 (treated with ZnNPs @5mg/ml), and T4 (treated with Ag/Cu/Zn nanocomposite @3.5mg/ml). The diabetes was induced by intraperitoneal injection of streptozotocin (@40mg/kg body weight) in experimental rats. Subsequently, a full thickness 10mm diabetic wound was induced on the dorsal lumber region of each rat, and treated with AgNPs, CuNPs, ZnNPs, and Ag/Cu/Zn nanocomposite-based ointments. The results revealed significant improvements ( $P < 0.05$ ) in wound contraction rate and reduced healing time in the T4 group treated with Ag/Cu/Zn nanocomposite ointment. Furthermore, histological analysis also showed a significant ( $P < 0.01$ ) effect on the formation of new epithelium, granulation tissue, angiogenesis, and collagen deposition in the T4 group treated with Ag/Cu/Zn nanocomposite ointment, resulting in diabetic wound regeneration. In conclusion, the Ag/Cu/Zn nanocomposite ointment not only promotes diabetic wound healing but also significantly improves the structural integrity of the regenerated tissue, highlighting its potential as an effective therapeutic option for diabetic wounds.

**To Cite This Article:** Murtaza G, Kausar R, Sial S, Hameed A, Rehan S, Kanwal A and Sharif MU, 2025. Targeting diabetic wound healing through tissue regeneration with silver, copper, and zinc nanoparticles in streptozotocin-induced diabetic albino rat model. Pak Vet J, 45(3): 1244-1252. <http://dx.doi.org/10.29261/pakvetj/2025.223>

#### INTRODUCTION

Diabetes mellitus (DM) is an endocrine disorder diagnosed by elevated blood glucose levels, resulting from impaired pancreatic insulin production or insulin resistance. It is also related to an incidence of microvascular problems, that pose a significant threat worldwide (Szlapinski and Hill, 2024). In DM, hyperglycemia damages blood vessels, nerves, and also affects tissue regeneration in diabetic wounds, where impaired blood circulation and reduced sensitivity increase the risk of infection and delay healing. Impaired wound healing in diabetic patients is influenced by both factors, such as infection, and systemic factors like hormonal

imbalance, which collectively hinder the process of wound regeneration (Ahmadieh-Yazdi *et al.*, 2024).

Diabetes is extremely prevalent, producing foot ulcers in 15% to 25% of an individuals and leading to amputations. Additionally, more than 85% of diabetic ulcerations result in lower limb amputations, indicating a worse prognosis (Yao *et al.*, 2024). Normal wound healing is an unpredictable process, involving the interactions between cells, growth factors, and cytokines. Therefore, diabetic wounds are more difficult to heal because of decreased cytokine responses, inadequate vascularization, and delayed healing processes (Singh *et al.*, 2023).

Local diabetic wound treatments are used to control bacterial infections, also promoting the wound

contraction rate by retaining moisture, and confiscating necrotic tissue (Tottoli *et al.*, 2020). Furthermore, numerous treatments have been suggested to enhance tissue regeneration in diabetic wound healing, but researchers are still very interested in using NPs to enhance tissue regeneration in diabetic wound healing due to their antioxidant, anti-inflammatory, and regenerative properties (Zheng *et al.*, 2024). In addition to promoting the reparative phase of healing such as granular tissue formation, collagen deposition, epithelial migration, extracellular matrix (ECM) remodeling, and angiogenesis, these NPs should also be able to modulate and unlock the inflammatory phase. Therefore, the innovation of new biomaterials and bioactive compounds is the key to the development of diabetic wound therapies. These innovative approaches are aimed at preventing the formation of ugly scars and helping wounds to heal faster by using NPs (Pérez-Díaz *et al.*, 2023). However, the regenerative potential of chemically synthesized NPs on diabetic wound healing has not been reported.

The current research investigates the therapeutic potential of chemically synthesized AgNPs, CuNPs, ZnNPs, and Ag/Cu/Zn nanocomposite on tissue regeneration in diabetic wound healing. Ultimately, the research provides insights into the selective potentials for AgNPs, CuNPs, ZnNPs, and Ag/Cu/Zn nanocomposite in their role as agents for tissue regeneration in diabetic wound healing. The current study has the specific purpose of forming a benchmark against which future works will analyze the toxicities of these NPs. The findings thus will not only promote a considerable global health burden, but they will also provide the way for developing treatment strategies for diabetic wound healing.

## MATERIALS AND METHODS

**Ethical Statement:** The research was approved by the Office of Research, Innovation, & Commercialization (ORIC), and the Institutional Biosafety, and Bioethics Committee (IBC), at the University of Agriculture, Faisalabad, Pakistan (Diary No. 3458/ORIC, dated June 10, 2024). All experimental procedures were conducted by the guidelines of National Biosafety Rules 2005 (Amended 2024)/Punjab Animal Health Act 2019, following the Bioethics Protocol.

**Nanoparticles Synthesis, and Characterizations:** AgNPs, CuNPs, and ZnNPs were synthesized by chemical reduction method, following the protocol described by (Khalid *et al.*, 2015; Quintero-Quiroz *et al.*, 2019). The reagents used for the synthesis of these NPs were purchased from the local market of Faisalabad. The synthesized NPs were further characterized by using X-ray Diffraction (XRD), Scanning Electron Microscopy (SEM) at the Government College University, Faisalabad, and Fourier Transform Infrared Spectroscopy (FTIR), Zeta Potential, UV-vis Absorption, Dynamic Light Scattering (DLS), at the University of Agriculture, Faisalabad, to confirmed the successful synthesis of desired NPs.

### In vivo Study

**Animal Housing and Management:** The 36 pathogen-free, healthy albino rats weighing 200 to 250 grams were purchased from the Institute of Physiology and

Pharmacology, University of Agriculture, Faisalabad. The rats were housed in standard environmental conditions i.e. constant temperature of  $21 \pm 2$  °C, humidity  $45 \pm 5\%$ , and light (12-hour light/dark cycle). The standard feed, clean water *ad libitum* were provided for the well-being of rats. Rats were acclimatized a week before the initiation of the experimental trial (National Research *et al.*, 2010).

**Experimental Design:** The rats were randomly divided into six different groups, each group contained six rats (n=6) as shown in Tab. 1. The group T0(CN) served as normal control, and T0(DC) as diabetic control. The groups T1, T2, and T3 were treated with the ointment of AgNPs @3mg/ml, CuNPs @2mg/ml, and ZnNPs @5mg/ml respectively, while the T4 group was treated with Ag/Cu/Zn nanocomposite ointment @3.5mg/ml.

**Table 1:** Experimental Design of Streptozotocin-Induced Diabetic Rat Model

Group	No of Rats	Experimental Design of Streptozotocin-Induced Diabetic Rat Model Treatment
T0 (NC)	6	Control Negative
T0 (DC)	6	Control Positive (Diabetic+Wound)
T1	6	Diabetic Wound+3mg/ml AgNPs ointment
T2	6	Diabetic Wound+2mg/ml CuNPs ointment
T3	6	Diabetic Wound+5mg/ml ZnNPs ointment
T4	6	Diabetic+Wound+3.5mg/ml Ag/Cu/Zn nanocomposite ointment

**Diabetic Rat Model:** The rats were given an intraperitoneal injection of streptozotocin (STZ) at @45 mg/kg body weight following a 12-hour fast, to induce experimental diabetes. After the STZ injection, the standard diet and sucrose water were provided to the rats (Akbarzadeh *et al.*, 2007). After four days, the blood glucose level was evaluated from the tail vein by using a glucometer. When the blood glucose levels in the rats increased more than 250 mg/dL, the rats were categorized as diabetic. Throughout the trial, blood glucose level was measured at baseline (day 0) and then on days 7, 14, and 23 post-wounding by using a glucometer.

**Excisional Wound Model:** The albino rats with confirmed DM were anesthetized with chloroform during the induction of the excisional wound. The dorsal hairs were removed, the underlying skin was wiped with 70% ethanol, and full thickness wounds (10mm) were generated on the dorsum of each rat by a surgical blade. At certain intervals, the contraction of the wound was recorded in mm (Pathak and Gadgoli, 2024).

**Nanoparticles Based Ointment Formation:** AgNPs, CuNPs, ZnNPs, and Ag/Cu/Zn nanocomposite-based ointment were prepared in petroleum jelly. Typically, in the first step, 30 grams of petroleum jelly was melted at 80°C in the water bath in four Petri dishes, and then @3mg of AgNPs, @2mg of CuNPs, @5mg of ZnNPs, and @3.5mg of Ag/Cu/Zn NPs were added separately in each 1ml of melted petroleum jelly. The four mixtures were homogenized by sonicating at 90°C for 40 minutes to achieve uniform dispersion. The resultant brownish-colored ointment of AgNPs, black-colored ointment of CuNPs, white-colored ointment of ZnNPs, and grayish-colored ointment of Ag/Cu/Zn nanocomposite were stored at 25°C for further use on diabetic wounds (Lisnawati *et al.*, 2019).

### Evaluation of Gross Morphological Parameters for Wound Healing

**Wound Contraction Rate:** The wound contraction rate was determined with a Vernier caliper on each observation day measured in mm. The contraction percentage will be calculated by using the following formula.

$\% \text{ Wound contraction} = \frac{A_z - A_t}{A_z} \times 100$  (Peng *et al.*, 2019) where "A<sub>t</sub>" is the wound area on corresponding days and "A<sub>z</sub>" is the wound area on day 0.

**Healing Time:** Healing time refers to the time of wound induction to the time of re-epithelization and tissue regeneration. Daily findings from day 0 to the end day of the experiment, healing rate were recorded. It was estimated by the sum of daily observations until the scar disappeared (Wang *et al.*, 2024).

**Histology of Wound:** At the end of the experimental period, the wounded skin tissue samples were collected, and processed by routine histological study. Hematoxylin, Eosin and Masson Trichrome stain were used to detect angiogenesis and collagen deposition. The histologically processed wounded tissue of every animal was examined using a compound microscope, and compared to samples from standard reference animals and control animals (Peng *et al.*, 2019).

**Statistical Analysis:** Statistical analysis was carried out by using one-way ANOVA and Tukey test (Minitab) so that  $P < 0.05$  was regarded as significant.

## RESULTS

### Characterization of NPs

**XRD of AgNPs, CuNPs, and ZnNPs:** The XRD spectra and diffraction peaks of chemically synthesized AgNPs, CuNPs, and ZnNPs are shown in Fig. 1 (a). The crystal size of AgNPs, CuNPs, and ZnNPs are calculated by using Scherrer's formula to indicate the successful synthesis of these NPs (Bayrami *et al.*, 2020). In the case of AgNPs, all the diffraction peaks are well aligned with JCPDS card number 00-040-1054, indicating a size of 9.86nm with a monoclinic crystalline structure. The XRD pattern of CuNPs displays fixed line widening of XRD diffraction peaks aligning with JCPDS card number 00-003-0898 indicating the size of 10.06nm with cubic crystal shape. On the other hand, the diffraction peaks of ZnNPs are well aligned with JCPDS card number 00-005-0664, indicating size of 9.07nm with spherical to hexagonal crystalline structure. All of the distinctive peaks confirmed the successful synthesis of AgNPs, CuNPs, and ZnNPs with no such impurities as shown in Fig. 1 (a).

**FTIR Analysis of AgNPs, CuNPs, and ZnNPs:** In FTIR analysis, the functional group of AgNPs, CuNPs, and ZnNPs is further studied in the range of 1000-4000 $\text{cm}^{-1}$  at room temperature as shown in Fig. 1 (b). In the case of AgNPs, the transmittance band situated at 3475-3570 $\text{cm}^{-1}$  indicating O-H stretching of water molecules. The band observed at 2338 $\text{cm}^{-1}$  is correlated with terminal alkyne groups, whereas the band observed at 1090 $\text{cm}^{-1}$ , and 879 $\text{cm}^{-1}$  indicated new C=C stretching and bonding in the

AgNPs. The band at 773 $\text{cm}^{-1}$  can be assigned to the existence of silver ions in the NPs arrangement. While the FTIR spectrum of CuNPs shows peaks at 3827 $\text{cm}^{-1}$ , assigned to the stretching of O-H of water molecules. The peak at 2338 $\text{cm}^{-1}$  in CuNPs suggests the existence of a carbon-carbon triple bond (C≡C) stretching vibration. The peak around 1120 $\text{cm}^{-1}$  and 1043 $\text{cm}^{-1}$  could be associated with the collective vibrations of Cu bonds in the CuNPs, and associated with C-H bending, while the 887 $\text{cm}^{-1}$  peak likely corresponds to the copper ions in CuNPs. Another hand, the FTIR spectra of ZnNPs materials show transmittance bands around 3576 $\text{cm}^{-1}$ , 3486 $\text{cm}^{-1}$ , 2360 $\text{cm}^{-1}$ , 1084 $\text{cm}^{-1}$ , 886 $\text{cm}^{-1}$ , and 762 $\text{cm}^{-1}$ . The strong peak at 1084 $\text{cm}^{-1}$  corresponds to the C-H band's deformation vibration, while the 762 $\text{cm}^{-1}$  band indicates the existence of zinc ions in the ZnNPs.

**Zeta Potential of AgNPs, CuNPs, and ZnNPs:** Zeta Potential demonstrates the stability of NPs for therapeutic application because stable NPs are typically more successful in biological systems. Fig. 1 (c) shows the zeta potential values of AgNPs, CuNPs, and ZnNPs, which are respectively, -21.1 mV, -11.1 mV, and -1.3 mV. Notice that, the NPs with more negative values indicate more stability, which means, the particles are less likely to aggregate, which is favorable for biological applications.

**UV-Vis Absorption Analysis of AgNPs, CuNPs, and ZnNPs:** UV-Vis spectroscopy is an approach used to determine the light absorbed and scattered by a given substance between 200 to 600nm in wavelength, which is used to confirm the physicochemical properties of AgNPs, CuNPs, and ZnNPs as shown in Fig.1 (d). The maximum absorption ( $\lambda_{\text{max}}$ ) spectrum of AgNPs showed broad a peak at 370nm in the visible light region. Monoclinic-shaped AgNPs would have distinct spectral behavior compared to spherical ones, UV-Vis absorption peak around 370nm, suggest that the AgNPs are smaller in size. The broad peak of the  $\lambda_{\text{max}}$  spectra of CuNPs was observed at 237nm, while the ZnNPs have  $\lambda_{\text{max}}$  spectra at 367nm, indicating successful synthesis of these NPs.

**DLS of AgNPs, CuNPs, and ZnNPs:** The DLS analysis revealed that the hydrodynamic diameters of AgNPs, CuNPs, and ZnNPs were 57nm, 64nm, and 75nm respectively as shown in Fig. 2 (a). The AgNPs had a diffusion coefficient of 1.4  $\mu\text{m}^2/\text{s}$  and a transmittance of 59.7%, and CuNPs had a diffusion coefficient of 0.8  $\mu\text{m}^2/\text{s}$  and a transmittance of 60.9%, while ZnNPs had a diffusion coefficient 3.4  $\mu\text{m}^2/\text{s}$  and transmittance of 59.8% at 25°C. The current study has established that AgNPs, CuNPs, and ZnNPs possess high physicochemical stability through hindering aggregation, and therefore increasing the physical stability, and purpose to use in biomedical applications.

**SEM Analysis of AgNPs, CuNPs, and ZnNPs:** The SEM analysis investigates the morphological and structural characteristics of the chemically synthesized AgNPs, CuNPs, and ZnNPs at 3 $\mu\text{m}$  magnifications respectively. In Fig. 2 (b) the SEM micrographs of AgNPs show a monoclinic crystalline structure with a crystalline size of 9.86 nm as documented in XRD crystallography. The SEM

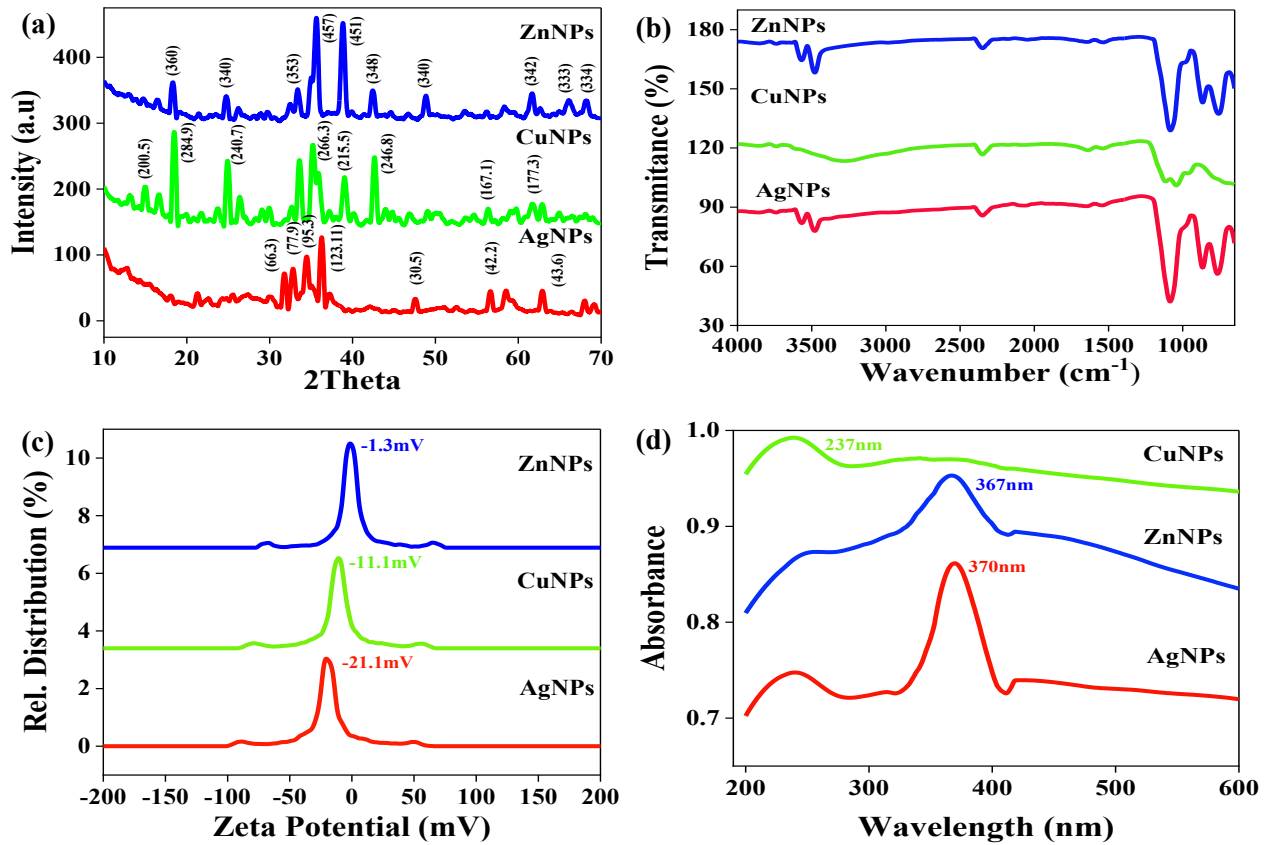


**Fig. 1:** (a) XRD Spectrum of AgNPs, CuNPs, and ZnNPs, (b) FTIR Analysis of AgNPs, CuNPs, and ZnNPs, (c) Zeta Potential of AgNPs, CuNPs, and ZnNPs, (d) UV-vis Absorption Analysis of AgNPs, CuNPs, and ZnNPs.

analysis of CuNPs revealed a cubic shape as depicted in Fig. 2 (c). These observations suggest the formation of nanostructured CuNPs with a range of morphologies and spatial arrangements with a particle size of 10.06 nm size. The SEM micrographs of ZnNPs demonstrate that the shape of the ZnNPs is hexagonal, with the crystalline size of 9.07 nm as shown in Fig. 2 (d).

### In vivo Wound Healing Activity

**Blood Glucose Levels in STZ-Induced Diabetic Rats:** Following STZ administration, blood glucose levels in the selected rats were monitored and documented in Table 2. Seven days post-induction, blood glucose levels exhibited a significant increase, exceeding 300 mg/dL. This hyperglycemia confirmed the successful induction of DM in the rats.

**Table 2:** Blood Glucose Level (mg/dL) in Streptozotocin-Induced Diabetic Rat Model

Groups	Blood Glucose (mg/dL) in Streptozotocin-Induced Diabetic Rat Model			
	Day 0	Day 7	Day 14	Day 23
T0 (CN)	105 ± 1	105 ± 1.5	106 ± 2	106 ± 1
T0(DC)	103 ± 9	279 ± 14*	320 ± 15**	372 ± 15***
T1	105 ± 7	271 ± 10*	331 ± 14**	378 ± 14***
T2	110 ± 2	281 ± 12*	319 ± 12**	357 ± 12***
T3	108 ± 2	268 ± 9*	321 ± 10**	382 ± 10***
T4	106 ± 1	273 ± 11*	301 ± 12**	339 ± 12***

The values are Means ± SD (n=3), \*\*\* P<0.001, \*\* P<0.01, \* P<0.05, are Statistically Significant.

### Gross Morphological Examination of Diabetic Wound

**Wound Contraction Percentage:** To assess the wound healing potential of AgNPs, CuNPs, ZnNPs, and Ag/Cu/Zn nanocomposite ointment, the wound contraction rate was measured in each rat at 5-days intervals. The results revealed

significant differences in wound contraction between the treatment groups across the healing period as shown in Fig. 3 (a &c). The T0(DC) group exhibits the slowest wound contraction rate throughout the experiment, and on day 25, they reach only about 51% wound closure, significantly lower than all other groups. This suggests the diabetic condition itself hinders the wound healing rate. The T1 and T2 groups show a similar pattern of wound contraction, significantly higher than T0(DC) but consistently lower than T4. By day 25, they achieved around 97% (T1) and 93% (T2) wound closure, indicating a substantial improvement as compared to the T0(DC) group. The T3 group shows moderate wound contraction of 82.75% by day 25 as compared to T0(DC) but less effective than T1 and T2. While the T4 group displays the fastest wound contraction rate, and by day 20, achieves complete wound closure (100%). This suggests the treatment with Ag/Cu/Zn nanocomposite ointment in the T4 group is the most effective in promoting wound healing as compared to T0(DC), AgNPs, CuNPs, and ZnNPs as shown in Fig. 3 (a &c).

**Healing Time of Diabetic Wound:** The data provided in Fig. 3 (b), the healing times (in days) for different groups labeled from T0(DC) to T4. The group T0(DC), shows the longest healing time, and remained unhealed at day 25, while the T1 group shows a shorter healing time of 21 days. There is a significant difference ( $P<0.01$ ) between T0(DC) and T1. The groups T1 and T2 have similar healing times and show no significant difference from each other, but are significantly different ( $P<0.05$ ) from T0(DC). The T3 group healed in 25 days, showing a significant difference ( $P<0.05$ ) between T0(DC), T1 and T2. Another hand, the T4 group has the shortest healing time of 18 days, showing a very highly

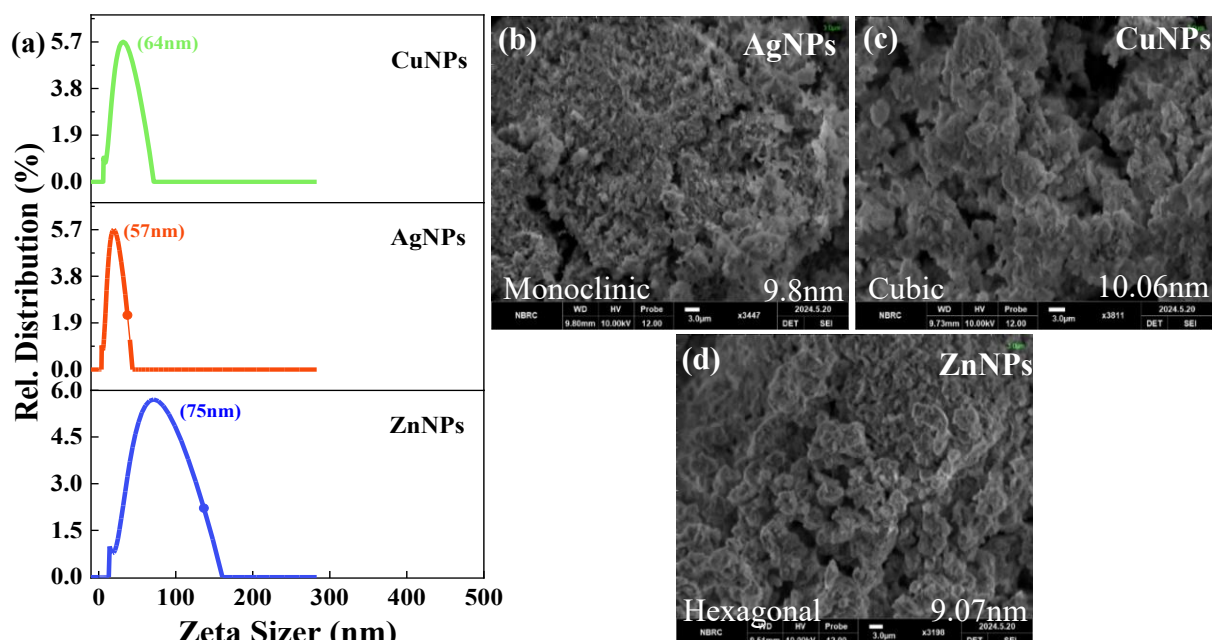


**Fig.2:** (a) Zeta sizer of AgNPs, CuNPs, ZnNPs, (b) SEM Analysis of AgNPs, (c) SEM Analysis of CuNPs (d) SEM Analysis of ZnNPs.

significant difference ( $P < 0.001$ ), from all other groups. This data suggests that the ointments AgNPs, CuNPs, and ZnNPs lead to faster healing times compared to the T0(DC), while the ointment of Ag/Cu/Zn nanocomposite is the most significantly effective in reducing healing time as shown in Fig. 3 (b).

### Histological Examination

**Regeneration of Epithelium, Granulation Tissue, and Blood Vessels in Diabetic Wound Healing:** Based on the histological analysis of wound, the Ag/Cu/Zn nanocomposite ointment appears to be the most effective treatment for wound regeneration as shown in Fig. 4 (a). In H&E staining, the T0(DC) group has the thickest epidermis, which may indicate prolonged inflammation and impaired healing. The groups T1, T2, and T3 show a statistically significant difference ( $P < 0.05$ ) but are less effective than T4 group. The T4 group shows a highly significant difference ( $P < 0.01$ ) by reducing epidermal thickness, suggesting better wound healing and remodeling as shown in Fig. 4(b). At day 25 post wounding, the T0(DC) has the worst regeneration score, confirming impaired healing. The T1, T2, and T3 groups show a significant difference ( $P < 0.05$ ), while the epidermal regeneration and remodeling of the dermis in T4 treated group were complete and highly significant ( $P < 0.01$ ) as compared to T0(DC) as shown in Fig. 4(c). The rats treated with Ag/Cu/Zn nanocomposite ointment (T4 group) displayed accelerated epidermal, dermal regeneration, and thinner epidermal thickness as compared with rats treated with AgNPs, CuNPs, ZnNPs as shown in Fig. 4(b & c). The T0(DC) group has excessive granulation tissue, which is a sign of delayed healing. The T1, T2 and T3 groups show a significant difference ( $P < 0.05$ ) by reducing granulation tissue as compared to T0(DC). The T4 group shows a highly significant difference ( $P < 0.01$ ), indicating that Ag/Cu/Zn nanocomposite ointment is the most effective treatment in reducing excessive granulation tissue as compared to the T0(DC) group as shown in Fig. 4(d). The T0(DC) group exhibits poor angiogenesis, confirming impaired healing in

diabetic wounds. The T1 and T2 groups show a significant difference ( $P < 0.05$ ), indicating a notable increase in angiogenesis. The T3 and T4 groups show a highly significant difference ( $P < 0.01$ ), suggesting in the T4 group the Ag/Cu/Zn nanocomposite ointment promotes the highest level of new blood vessel formation as shown in Fig. 4(e). The Ag/Cu/Zn nanocomposite ointment significantly enhances blood vessel formation, making it the most effective treatment for improving angiogenesis and wound healing.

### Regeneration of Collagen Fibers in Diabetic Wound Healing:

Diabetic wound healing is mainly dependent on collagen deposition, therefore to investigate the effect of NPs on collagen deposition, skin samples of rats were stained with Masson Trichrome as shown in Fig. 5(a). The staining results revealed that the collagen deposition was significantly higher in the Ag/Cu/Zn nanocomposite ointment-treated group (T4). The AgNPs (T1) and CuNPs (T2) groups significantly ( $P < 0.01$ ) enhance collagen deposition in diabetic wounds compared to the T0(DC). The ZnNPs (T3) and Ag/Cu/Zn nanocomposite (T4) groups seem to be the most significantly ( $P < 0.001$ ) effective treatments for promoting collagen deposition. The results indicated that the Ag/Cu/Zn nanocomposite ointment group had the greatest collagen deposition, the least in AgNPs, and CuNPs, while moderate in ZnNPs groups as compared to T0(DC) group as shown in Fig. 5(b).

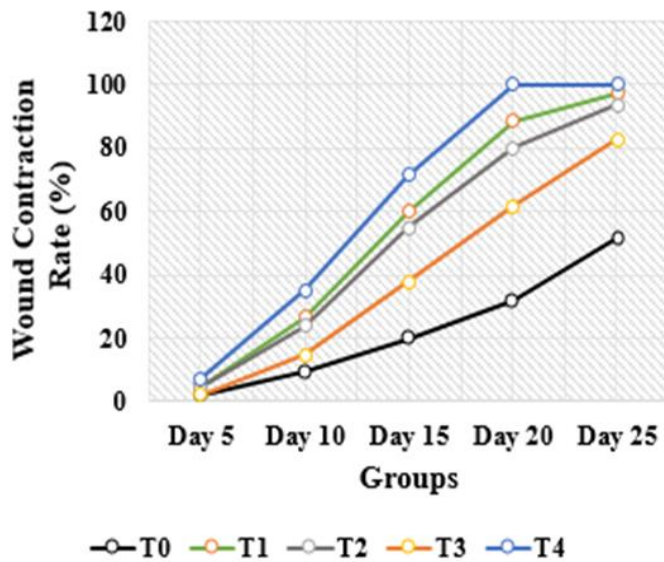
## DISCUSSION

Tissue regeneration is essential for diabetic wound healing, which involves keratinocyte proliferation, angiogenesis, and collagen deposition. The NPs have the regenerative potential, regarded as safe for humans and animals (Choudhury *et al.*, 2020). There was a need to know the regenerative potential of chemically synthesized AgNPs, CuNPs, ZnNPs, and Ag/Cu/Zn nanocomposite against diabetic wounds healing in-vivo in a rat's model, which had been evaluated in this study. Therefore, the results of these

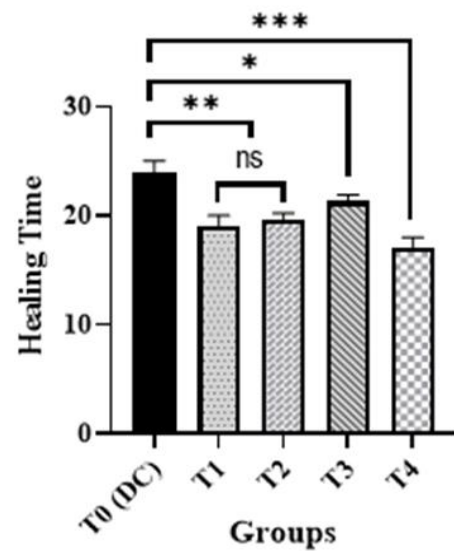
NPs based ointments have been compared, due to their higher susceptibility towards diabetic wound healing. In our study, the Ag/Cu/Zn nanocomposite ointment showed significantly ( $P < 0.001$ ) higher regenerative potential toward diabetic wound healing than AgNPs, CuNPs, and ZnNPs. Similarly, Bayrami *et al.* (2020) comparatively studied the potential of biologically synthesized ZnO/CuO/Ag nanocomposite using propolis extract for wound healing in Iran and found that ZnO/Ag/Ext NPs accelerate wound healing and upsurge wound contraction rate (Bayrami *et al.*, 2020). Thus, one of the goals of this research was to contribute to the intention toward the chemically synthesized NPs, because, to our best knowledge, these NPs have not been used in-vivo in diabetic

wound healing. In this study, AgNPs, CuNPs, and ZnNPs were chemically synthesized, characterized for quality assessment, and incorporated into an ointment for testing on streptozotocin-induced diabetic rat model. The average crystal size of AgNPs was 9.8nm with distinct monoclinic shape, CuNPs was 10.06nm with cubic shape, and ZnNPs was 9.07nm with hexagonal shape as shown in Fig 1(a) and Fig. 2 (b,c,d), exist under the category of NPs as previously documented by (Khalid *et al.*, 2015; Ehsan and Sajjad, 2017; Quintero-Quiroz *et al.*, 2019). FTIR analysis confirmed the functional groups of these NPs, and the FTIR spectra of AgNPs are corresponding with (Kantipudi *et al.*, 2018), CuNPs are corresponding with (Javed *et al.*, 2017),

(a) Wound Contraction Rate (%) of Diabetic Wounds in Streptozotocin-Induced Diabetic Rat Model



(b) Healing Time of Diabetic Wound in Streptozotocin-induced Diabetic Rats Model



(c) Photographic Representation of Wound Healing in Streptozotocin-Induced Diabetic Rat Model

Groups	Photographic Representation of Wound Healing in Streptozotocin-Induced Diabetic Rat Model				
	Day 5	Day 10	Day 15	Day 20	Day 25
T0					
T1					
T2					
T3					
T4					

Fig.3: (a) Wound Contraction Percentage of Diabetic Wound, (b) Healing Time of Diabetic Wound, (c) Photographic Representation of Wound at Different Time Intervals in Streptozotocin-Induced Diabetic Rat Model.

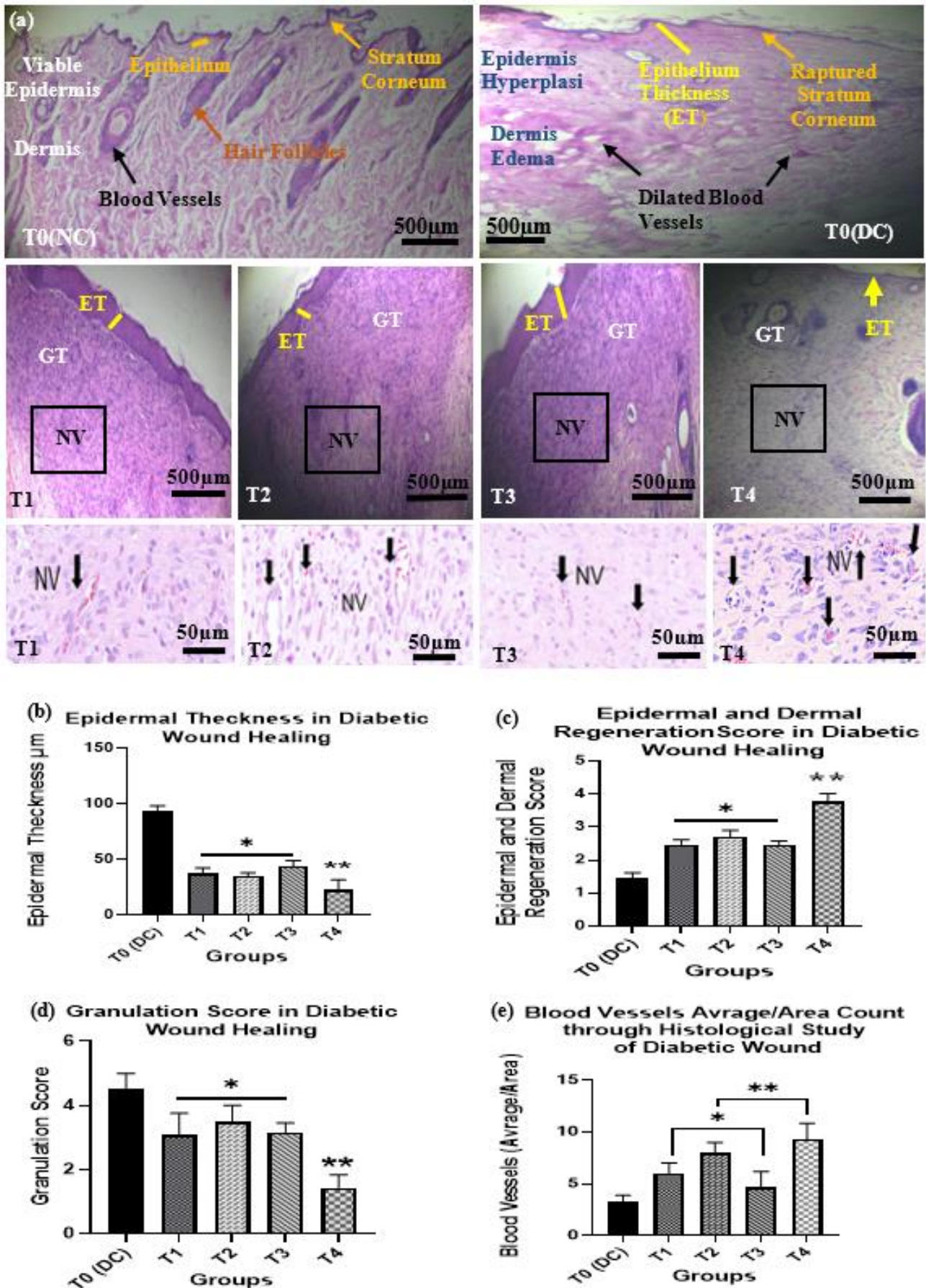


**Fig.4:** (a) Post-Treatment H&E Staining of Wound Tissues showing Epidermal Thickness (ET), New Granulation Tissue (GT), and New Blood Vessels (NV). Yellow lines indicate Epidermal Thickness, Black Circles and Black Thick Arrows indicate New Blood Vessels and GT indicates Granulation Tissue Respectively, (b) Epidermal Thickness, (c) Epidermal and Dermal Regeneration Score, (d) Granulation Score, and (e) Blood Vessels Average/Area Count through Histological Study of Diabetic Wound Healing.

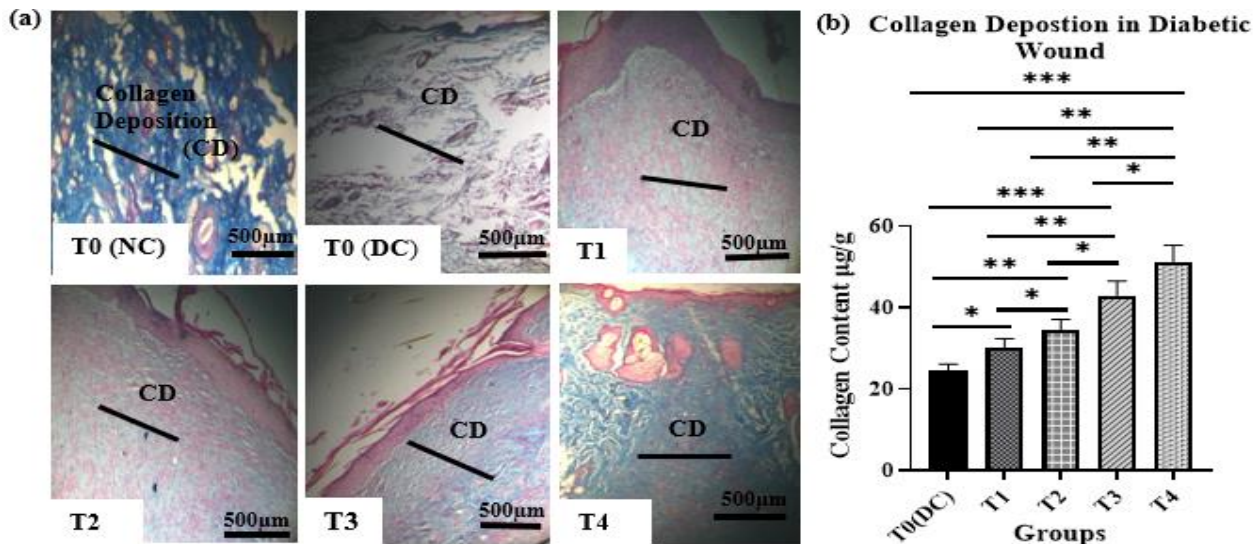


**Fig.5:** (a) Masson Trichrome Staining of Wound Tissues Post-Treatment, Collagen was Stained Blue-Green, whereas the Cytoplasm, Red Blood Cells, and Muscle were Stained Red, (b) Collagen Deposition in Diabetic Wound Healing.

and ZnNPs are corresponding with (Bayrami *et al.*, 2018). UV-Vis spectral analysis provided further confirmation, with the maximum absorbance peak ( $\lambda_{max}$ ) at 380nm for AgNPs, 355nm for CuNPs, and 238nm for ZnNPs, all these absorbance peaks are in accordance with values already reported in the literature by (Al-thabaiti *et al.*, 2015; Arvanag *et al.*, 2019; Furqon *et al.*, 2021). DLS measurements also showed hydrodynamic diameters of the synthesized NPs. The average hydrodynamic diameter of AgNPs was 356.4nm, CuNPs was 642.5nm, and ZnNPs was 144.22nm, confirming their stability and suitability for biomedical applications. These results support the successful synthesis of these NPs as documented by (Khalid *et al.*, 2015; Ehsan and Sajjad, 2017; Quintero-Quiroz *et al.*, 2019). These physicochemical properties contribute to the regenerative potential of the NPs and provide a robust foundation for exploring their therapeutic efficacy in diabetic wound healing. Similarly, Thanusha *et al.* (2018) successfully synthesized CuO and ZnONPs containing hydrogel, demonstrating its potential to promote wound healing in Wistar rats (Thanusha *et al.*, 2018).

Diabetes, a global health issue, has emerged as one of the major questions of concern among all intellectuals. Wound healing in diabetes is blunted due to issues such as inflammation, and poor angiogenesis (Singh *et al.*, 2023). The rats were randomly divided into six different groups, and diabetic wounds were induced in each group to assess wound healing. The Ag/Cu/Zn nanocomposite ointment significantly ( $P < 0.001$ ) promoted wound contraction and reduced the wound healing time in the T4 group as compared to the group T0(DC), and own better wound contraction as shown in Fig 3 (a & c). Our results are aligning with Bayrami *et al.* (2020), who reported a significant ( $P < 0.05$ ) wound closure rate in ZnO/Ag/Ext treated wounds at day 18<sup>th</sup> as compared to the other groups (Bayrami *et al.*, 2020).

Histological analysis revealed fast re-epithelialization and collagen deposition in treated wounds as shown in Fig 4 & 5. Re-epithelialization is a significant phase in wound healing and involves the immigration of keratinocytes over the wound surface to restructure the epidermis. In the present study, the Ag/Cu/Zn nanocomposite enhanced wound healing and promoted re-epithelialization in the T4 group.

Kantipudi *et al.*, (2018), documented that, the composite of AgNPs and ZnONPs promotes maximum wound-healing efficiency, due to the rapid epithelialization of skin in Wister rat (Kantipudi *et al.*, 2018).

Another prerequisite to adequate wound healing is the controlled synthesis and deposition of collagen. As highlighted by Rath *et al.* (2016), NPs promote keratinocyte activity, ECM remodeling, and collagen synthesis, during the initial phases of wound healing (Rath *et al.*, 2016). In the current study, the T0(DC) group showed less collagen deposition in the diabetic wounds, thus having less granulation tissue formation, while AgNPs, CuNPs, ZnNPs, particularly Ag/Cu/Zn nanocomposite, stimulate collagen deposition, and granulation tissues formation, support healthy wound healing as depicted in Fig. 4(d) & 5(a & b). It was previously demonstrated by Wang *et al.* (2020), AgNPs, and CuNPs nanocomposite enhanced collagen deposition during the wound healing (Wang *et al.*, 2020).

Diabetic wounds were also characterized by poor blood vessel formation; therefore, angiogenesis was examined by histological analysis in our study. The Ag/Cu/Zn nanocomposite had a more pronounced effect on promoting angiogenesis required for tissue regeneration as shown in Fig. 4(e). This result is consistent with the study of Khalkhali *et al.* (2025), who reported that copper and magnesium hybrid promotes angiogenesis in vivo and in vitro investigation (Khalkhali *et al.*, 2025). The increased angiogenesis in T4 group indicates that the NPs-mediated therapy may well fill the vascular deficits and improve the diabetic wound healing. Similarly, Xiao *et al.* (2017), prepared copper-based hydrogel to improve diabetic wound healing possibly by promoting angiogenesis (Xiao *et al.*, 2017).

The individual contributions of each NPs in diabetic wound healing were accessed. AgNPs exhibited antimicrobial activity, reducing bacterial burden and making a conducive environment for healing (Furqon *et al.*, 2021). CuNPs promoted angiogenesis, keratinocyte proliferation, collagen synthesis, and ECM remodeling (Gopal *et al.*, 2014), while ZnNPs enhanced epithelial repair and tissue stability (Kumar *et al.*, 2019). The synergistic interaction between these components likely underpins the superior efficacy of the nanocomposite compared to individual

treatments with these NPs. Similarly, Lu *et al.* (2017) conducted in vivo research in mice and found that Chitosan-Ag/Zn dressings promoted more efficient re-epithelialization, denser collagen deposition, and accelerated wound healing compared to pure Zn and chitosan dressing ointment gauze (Lu *et al.*, 2017).

The findings of this study highlight the potential of Ag/Cu/Zn nanocomposite ointment as an effective therapeutic strategy for diabetic wound management. The nanocomposite ointment addresses key aspects of impaired healing, including inflammation, re-epithelialization, collagen deposition, and angiogenesis. Further research should focus on elucidating the specific molecular mechanisms underlying the observed synergistic effects and conducting advanced preclinical and clinical trials to establish safety and efficacy in more complex biological environments.

**Conclusion:** In this study, the AgNPs, CuNPs, and ZnNPs, particularly when combined in Ag/Cu/Zn nanocomposite ointment, can promote diabetic wound regeneration by targeting multiple phases of wound healing. This data indicates that the Ag/Cu/Zn nanocomposite ointment regenerates wounds by promoting wound contraction, collagen deposition, re-epithelialization, and angiogenesis in treated rats. These findings suggest that chemically synthesized NPs based treatment is a promising novel therapeutic strategy for diabetic wound healing, which could also be used in combination with other wound healing therapies. Further studies on their safety, long-term effects, and optimal delivery mechanisms will be valuable in realizing the clinical potential of these formulations in diabetic wound management.

**Contribution of authors:** Dr. Razia, Dr. Shahnawaz and Ghulam Murtaza and Dr. Amjad design this research project, with the expert opinion of Dr. Aneela. Dr Sarmad helped in statistical modelling, and Umar sharif help in reviewing this article.

## REFERENCES

- Ahmadieh-Yazdi A, Karimi M, Afkhami E, *et al.*, 2024. Unveiling therapeutic potential: Adipose tissue-derived mesenchymal stem cells and their exosomes in the management of diabetes mellitus, wound healing, and chronic ulcers. *Biochem Pharmacol* 11:63-99.
- Akbarzadeh A, Norouzzian D, Mehrabi MR, *et al.*, 2007. Induction of diabetes by streptozotocin in rats. *Indian J Clin Biochem* 22:60-4.
- Al-Thabaiti SA, Obaid AY, Khan Z, *et al.*, 2015. Cu nanoparticles: synthesis, crystallographic characterization, and stability. *Colloid Polym Sci* 293:2543-55.
- Arvanag FM, Bayrami A, Habibi-Yangjeh A, *et al.*, 2019. A comprehensive study on antidiabetic and antibacterial activities of ZnO nanoparticles biosynthesized using *Silybum marianum* L seed extract. *Mater Sci Eng C* 97:397-405.
- Bayrami A, Parvinroo S, Habibi-Yangjeh A, *et al.*, 2018. Bio-extract-mediated ZnO nanoparticles: microwave-assisted synthesis, characterization and antidiabetic activity evaluation. *Artif Cells Nanomed Biotechnol* 46:730-9.
- Bayrami M, Bayrami A, Habibi-Yangjeh A, *et al.*, 2020. Biologically-synthesized ZnO/CuO/Ag nanocomposite using propolis extract and coated on gauze for wound healing applications. *IET Nanobiotechnol* 14:548-54.
- Choudhury H, Pandey M, Lim YQ, *et al.*, 2020. Silver nanoparticles: advanced and promising technology in diabetic wound therapy. *Mater Sci Eng C* 112:1109-25.
- Ehsan S and Sajjad M, 2017. Bioinspired synthesis of zinc oxide nanoparticles and its combined efficacy with different antibiotics against multidrug-resistant bacteria. *J Biomater Nanobiotechnol* 8:1-10.
- Furqon IA, Hikmawati D, Abdullah C, *et al.*, 2021. Antibacterial properties of silver nanoparticle (AgNPs) on stainless steel 316L. *Nanomed Res J* 6:117-27.
- Gopal A, Kant V, Gopalakrishnan A, *et al.*, 2014. Chitosan-based copper nanocomposite accelerates healing in excision wound model in rats. *Eur J Pharmacol* 731:8-19.
- Javed R, Ahmed M, ul Haq I, *et al.*, 2017. PVP and PEG doped CuO nanoparticles are more biologically active: Antibacterial, antioxidant, antidiabetic and cytotoxic perspective. *Mater Sci Eng C* 79:108-15.
- Kantipudi S, Sunkara JR, Rallabhandi M, *et al.*, 2018. Enhanced wound healing activity of Ag-ZnO composite NPs in Wistar Albino rats. *IET Nanobiotechnol* 12:473-8.
- Khalid H, Shamaila S, Zafar N, *et al.*, 2015. Synthesis of copper nanoparticles by chemical reduction method. *Sci Int* 27:3085-8.
- Khalkhali P, Omidi M, Masson-Meyers DS, *et al.*, 2025. Promoting angiogenesis/osteogenesis by a new copper/magnesium hydroxide hybrid nanoparticle: In vitro and in vivo investigation. *J Biomed Mater Res A* 113:378-55.
- Kumar S, Lakshmanan V-K, Raj M, *et al.*, 2019. Evaluation of wound healing potential of chitin hydrogel/nano zinc oxide composite bandage. *Pharm Res* 36:523-30.
- Lisnawati N, Kumala S and Rahmat D, 2019. Formulation and evaluation of antibacterial activity of nanoparticles ointment preparation using Blimbi extract. *Pharm Biomed Res*, 4(3): 32-39.
- Lu Z, Gao J, He Q, *et al.*, 2017. Enhanced antibacterial and wound healing activities of microporous chitosan-Ag/ZnO composite dressing. *Carbohydr Polym* 156:460-9.
- National Research Council (US) Committee for the Update of the Guide for the Care and Use of Laboratory Animals. *Guide for the Care and Use of Laboratory Animals*. 8th edition. Washington (DC): National Academies Press (US); 2011. Available from: <https://www.ncbi.nlm.nih.gov/books/NBK54050/> doi: 10.17226/12910.
- Pathak PC and Gadgoli CH, 2024. Exploring the efficacy of *Panchavalk* extract and zinc-copper *Bhasma* in promoting wound healing in incision and excision wound models in the rat. *J Ethnopharmacol* 320:117404.
- Peng Y, Wu S, Tang Q, *et al.*, 2019. KGF-1 accelerates wound contraction through the TGF- $\beta$ 1/Smad signaling pathway in a double-paracrine manner. *J Biol Chem* 294:8361-70.
- Pérez-Díaz MA, Prado-Prone G, Díaz-Ballesteros A, *et al.*, 2023. Nanoparticle and nanomaterial involvement during the wound healing process: an update in the field. *J Nanopart Res* 25:27.
- Quintero-Quiroz C, Acevedo N, Zapata-Giraldo J, *et al.*, 2019. Optimization of silver nanoparticle synthesis by chemical reduction and evaluation of its antimicrobial and toxic activity. *Biomater Res* 23:27.
- Rath G, Hussain T, Chauhan G, Garg T and Goyal AK, 2016. Collagen nanofiber containing silver nanoparticles for improved wound-healing applications. *J Drug Target* 24(6): 520-529.
- Singh SK, Dwivedi SD, Yadav K, *et al.*, 2023. Novel biotherapeutics targeting biomolecular and cellular approaches in diabetic wound healing. *Biomed* 11:61-3.
- Szlapinski SK and Hill DJ, 2024. In vivo models of gestational and type 2 diabetes mellitus characterized by endocrine pancreas cell impairments. *J Endocrinol* 260:1-9.
- Thanusha AV, Dinda AK and Koul V, 2018. Evaluation of nano hydrogel composite based on gelatin/HA/CS suffused with Asiatic acid/ZnO and CuO nanoparticles for second-degree burns. *Mater Sci Eng C* 89:378-86.
- Tottoli EM, Dorati R, Genta I, *et al.*, 2020. Skin wound healing process and new emerging technologies for skin wound care and regeneration. *Pharm* 12:73-5.
- Wang J, He J, Yang Y, *et al.*, 2024. Hemostatic, antibacterial, conductive and vascular regenerative integrated cryogel for accelerating the whole wound healing process. *Chem Eng J* 479:1475-77.
- Wang K, Pan S, Qi Z, *et al.*, 2020. Recent advances in chitosan-based metal nanocomposites for wound healing applications. *Adv Mater Sci Eng* 2020:38279-12.
- Xiao J, Chen S, Yi J, *et al.*, 2017. A cooperative copper metal-organic framework-hydrogel system improves wound healing in diabetes. *Adv Funct Mater* 27:16048-72.
- Zheng Q, Chen C, Liu Y, *et al.*, 2024. Metal nanoparticles: advanced and promising technology in diabetic wound therapy. *Int. J. Nanomed* 19:965-92.